Correlation between onset of yielding and free volume in metallic glasses

J.G. Wang,[a] D.Q. Zhao,[a] M.X. Pan,[a] W.H. Wang,[a,*] S.X. Song[b] and T.G. Nieh[b]

[a]*Institute of Physics, Chinese Academy of Sciences, Beijing 100190, China*
[b]*Department of Materials Science and Engineering, The University of Tennessee, Knoxville, TN 37996-2200, USA*

Based on the free volume model, a critical value of reduced free volume is proposed to be the sufficient condition for the onset of yielding in metallic glasses. The corresponding stress for the onset of yielding is found to be less than the macroscopically measured yield strength, which is consistent with experimental observations. The difference in deformability between brittle and plastic metallic glasses can be explained in terms of the free volume evolution in the localized shear zone.
© 2009 Acta Materialia Inc. Published by Elsevier Ltd. All rights reserved.

In the field of metallic glass (MG) science, major attention has been focused on the understanding of plastic deformation, because plasticity is highly desired to meet engineering needs [1–9]. Recently, the development of malleable MGs made easy the investigation of the process and mechanism of the plastic deformation of MGs [6,7]. A malleable MG, when compressed or rolled, can be considered as an elastic–plastic material which can flow plastically under macroscopic yield stress σ_y due to the absence of strain hardening [5]. Yielding, therefore, is regarded as a transition point between the elastic strain and the plastic strain in MGs. Interestingly, there have been sporadic reports that the onset of yielding in MGs actually takes place below the experimentally macroscopic yield strength [7]. For example, Park et al. [4,8] conducted creep experiments on MG at room temperature and showed that deformation could proceed at $0.9\sigma_y$, without apparent formation of shear bands. Chen et al. [7] also demonstrated that yielding can take place in MGs at a stress level as low as $0.8\sigma_y$. However, the nature of yielding in MGs received little attention.

For crystalline materials, the macroscopic yielding had been extensively studied and several well-known yield criteria were developed [5]. The onset of yielding marks the motion of dislocations at the atomic scale. When a shear stress τ is applied to a material, two internal stresses will respond: long-range internal stress τ_G, which is mainly determined by the shear modulus G, and short-range internal stress τ_p, which mainly comes from the Peierls stress, localized in less than 10 atom diameters scale [5]. In the case of MGs, since there is no long-range ordered microstructure, the long-range internal stress is absent and only the short-range stress operates. Two models, free volume [10] and shear transformation zone (STZ) [11], were proposed to explain the plastic flow of MGs. The STZ theory suggests that a flow event is initiated from rearrangements of atoms in local regions which contain tens or hundreds of atoms [12,13]. However, a full description of cooperative motion of hundreds of atoms is mathematically too difficult to obtain. In contrast, free volume theory deals with only several atoms around an open site which is much easier to treat mathematically [10]. However, earlier studies of the deformation of MGs based on the free volume model were primarily on the plastic flow. Limited work has been carried out in the elastic region and the onset of yielding of MGs [4]. In this work, we reexamine the concept of elastic strain and the onset of yielding of the MGs, and a critical value of free volume is proposed to be a sufficient condition for the yielding in MGs.

In the free volume model, the net rate of increase of the average free volume per atom, v_f, is the difference between the increase rate of v_f caused by shear-induced dilatation and the decreasing rate of v_f caused by diffusion-induced annihilation [10]:

$$\dot{x} = \frac{f}{\alpha v^*} \exp\left(-\frac{\Delta G^m}{kT}\right) \exp\left(-\frac{1}{x}\right)\left\{\frac{2kT}{S}\frac{1}{x}\left[\cosh\left(\frac{\tau\Omega}{2kT}\right) - 1\right] - \frac{v^*}{n_D}\right\}$$

(1)

where the reduced free volume (RFV) $x = \frac{v_f}{\alpha v^*}$ is introduced, because the absolute value of v_f is hard to obtain [12]. f is the frequency of atomic vibration ($\sim$Debye frequency), α is a geometric factor between 0.5 and 1, v^* is the critical (hard-sphere) volume of an atom, k is the Boltzmann constant, T is the temperature, Ω is the atomic volume ($\sim 1.25v^*$), ΔG^m is the activation energy of atomic motion, and $S = \frac{2}{3}G\frac{1+\mu}{1-\mu}$, where μ is Poisson's ratio, n_D is the number of diffusive jumps to annihilate a free volume equal to v^*, which is between 1 and 10.

To understand the evolution of free volume and the yielding of MGs, numerical calculations were carried out using Eq. (1). It is pointed out that the stress loading rate is $2.6G \times 10^{-4}\,\text{s}^{-1}$ before the applied stress τ reaches yield shear stress τ_y ($\sim\sigma_y/2$). After that, the applied stress keeps a constant value, τ_y. However, the activation energy ΔG^m and the initial value of RFV x_0 need to be determined first. ΔG^m is roughly estimated to be (i) nhf ($n = 1, 2\ldots$, and h is Planck's constant) when the atom is dealt with as a three-dimensional isotropic oscillator and (ii) $(8/\pi^2)G\gamma_C^2\zeta\Omega_s$ ($\gamma_c \sim 0.026$, $\zeta \sim 3$, $\Omega_s \sim 2v^*$ here) proposed by Johnson [12]. The glassy alloy $Zr_{46.7}Ti_{8.3}Cu_{7.5}Ni_{10}Be_{27.5}$ (Vit4), for example, has a density change of $\sim$1% after annealing [14]. If the increment of density is entirely ascribed to the annihilation of free volume, the x_0 for Vit4 would be on the order of $\sim$1% (α taken to be 1). Figure 1 presents the numerical results using the parameters listed in Table 1. Here, we adopt x_0 to be 2.2% for two reasons: (1) a smaller x_0, for example, 1.0% or 1.5%, needs a geological timescale for the evolution of FRV to produce a change, which is incon-

sistent with experimental observations; (2) The probability $p(x)dx$ of finding an atom with RFV between x and $x + dx$ is: $p(x)dx = c_1 \exp(-c_2x)dx$ [10], where c_1 and c_2 are constant, so x_0 can be taken to 2.2%, only with a lower possibility than 1.0%. The calculated results for $Fe_{53}Cr_{15}Mo_{14}Er_1C_{15}B_6$ (Fe-MG), $Zr_{55}Ti_5Cu_{20}Ni_{10}Al_{10}$ (Zr-MG), and $Pt_{57.5}Cu_{14.7}Ni_5P_{22.8}$ (Pt-MG) with $\Delta G^m = hf$, $\alpha = 1$ and $n_D = 3$ are shown in Figure 1a. It can be observed that the RFV sharply increases when it reaches a critical value of about 2.4%, which appears to be independent of the chemical composition and mechanical parameters of the different MGs. The evolution of RFV in the Zr-MG with $\alpha = 1$, $n_D = 3$, and $\Delta G^m = (8/\pi^2)G\gamma_C^2\zeta\Omega_s$, hf, $2hf$, respectively, is shown in Figure 1b. Again, x increases sharply at the same critical value x_C of $\sim$2.4%, independent of the ΔG^m. Numerical results also show that the critical value of RFV is independent of n_D, α and x_0. In summary, the critical value of $\sim$2.4% appears to be universal for MGs.

The rapid increase in free volume over x_C will drastically reduce the viscosity and the shear resistance of the alloy [10], thus causing the yielding of the sample. This, in fact, has been confirmed by MD simulation and elastostatic compression [4]. Since a MG is expected to yield as the RFV reaches the critical value x_C, this effective stress may not necessarily correspond to the experimentally measured macroscopic yield stress (or the strength). To estimate the effective stress, we now turn our attention to the free volume evolution.

In principle, during deformation, the free volume gradually increases (i.e., $\dot{x} > 0$) until it reaches x_C, at which $\dot{x} = 0$ and the shear stress τ reaches a critical value τ_c.

This critical shear stress is determined from Eq. (1) as

$$\tau_c = \frac{2kT}{\Omega}\cos h^{-1}\left(\frac{x_C S}{2kT}\frac{v^*}{n_D} + 1\right)$$

(2)

Substituting $x_C \sim 2.4\%$ into Eq. (2), τ_c can be obtained according to the parameters listed in Table 1 (n_D and T taken to be 3 and 300 K, respectively). The calculated σ_c ($\sim 2\tau_c$) and σ_y of a number of BMGs are listed in Table 1 [15–18]. It is apparent that $\sigma_c < \sigma_y$, which is consistent with the notion that the very stress for the onset of yielding is usually smaller than the macroscopic yield strength [4,7,8]. This demonstrates that when a stress satisfying Eq. (2) is applied, x will grow to $\sim$2.4%, and the sample will yield, provided it is loaded for a sufficiently long time. Figure 2 exhibits the evolution of x in a Zr-MG under three different applied stresses of 1.6 GPa ($\sim\sigma_y$, red curve), 1.2 GPa ($\sim 0.8\sigma_y$, blue curve) and 1.0 GPa ($\sim 0.6\sigma_y$, green curve). It is clear that a smaller applied stress σ requires a longer loading time for x to reach x_C.

Although the physical explanation for the existence of the critical value of RFV is unclear, an analogy can be made. For 0.35 wt.% carbon steel and pure lead, volume expansion at melting are $\sim$3.0% and $\sim$3.2%, which are close to 2.4%. It is pointed out that the x cannot exceed a maximum value x_m, for the alloy would transit into liquid state or suffer a failure when $x > x_m$. For example, the 0.35 wt.% carbon steel would be melted if thermal expansion was over $\sim$3%. Therefore, if $x_C < x < x_m$, the MG would be in the supercooled liquid
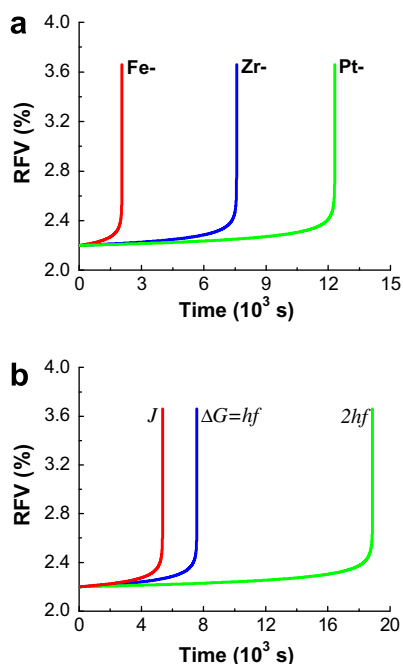

Figure 1. The evolution of RFV in specimens under shear (otherwise you must specify the stress value) with time, and the parameters $\alpha = 1$ and $n_D = 3$. (a) Three typical MGs, i.e., Fe, Zr, Pt, with $\Delta G^m = hf$. (b) The Zr-MG with different $\Delta G^m s$ ($J = (8/\pi^2)G\gamma_C^2\zeta\Omega_s$).

Table 1. Data of average atomic volume v^*, Poisson's ratio μ, shear modulus G, Debye frequency f, and yield stress σ_y, and the critical stress σ_c of 32 MGs used in Figures 1 and 2 are from Refs. [12,15–18].

Alloy composition	v^* (10^{-29} m^3)	μ	G (GPa)	f (10^{12}Hz)	σ_y (GPa)	σ_c (GPa)
1. $Ca_{65}Zn_{16.5}Mg_{8.5}Li_{10}$	3.362	0.306	8.9	4.595	0.53	0.33
2. $Ce_{70}Al_{10}Ni_{10}Cu_{10}$	2.813	0.313	11.5	2.997	0.65	0.41
3. $La_{55}Al_{25}Cu_{10}Ni_5Co_5$	2.639	0.342	15.6	3.773	0.85	0.50
4. $Mg_{65}Cu_{25}Gd_{10}$	1.949	0.320	18.6	5.539	0.98	0.63
5. $La_{55}Al_{25}Co_{20}$	2.718	0.327	15.4	3.769	0.99	0.48
6. $Au_{55}Cu_{25}Si_{20}$	1.767	0.417	24.6	3.837	1.00	0.83
7. $Pr_{55}Al_{25}Co_{20}$	2.502	0.324	17.4	3.927	1.01	0.53
8. $Au_{49.5}Ag_{5.5}Pd_{2.3}Cu_{26.9}Si_{16.3}$	1.748	0.406	26.5	4.093	1.20	0.86
9. $Pt_{60}Ni_{15}P_{25}$	1.413	0.420	33.8	4.274	1.40	1.09
10. $Cu_{46}Zr_{54}$	1.711	0.391	30.0	5.401	1.40	0.90
11. $Pt_{57.5}Cu_{14.7}Ni_5P_{22.8}$	1.437	0.434	33.4	4.302	1.45	1.09
12. $Pd_{77.5}Cu_6Si_{16.5}$	1.452	0.409	31.8	5.040	1.50	1.03
13. $Pd_{64}Ni_{16}P_{20}$	1.376	0.405	32.7	5.277	1.55	1.07
14. $Zr_{57.5}Nb_5Cu_{15.5}Ni_{12}Al_{10}$	1.959	0.379	30.8	5.654	1.58	0.84
15. $Cu_{46}Zr_{42}Al_7Y_5$	1.698	0.364	31.0	5.630	1.60	0.89
16. $Zr_{55}Ti_5Cu_{20}Ni_{10}Al_{10}$	1.852	0.375	31.0	5.724	1.63	0.86
17. $Zr_{64.13}Cu_{15.75}Ni_{10.12}Al_{10}$	1.939	0.377	28.5	5.415	1.69	0.81
18. $Pd_{60}Cu_{20}P_{20}$	1.405	0.409	32.3	5.295	1.70	1.06
19. $Pd_{40}Cu_{30}Ni_{10}P_{20}$	1.319	0.399	34.5	5.725	1.72	1.12
20. $Pd_{40}Cu_{40}P_{20}$	1.325	0.402	33.2	5.609	1.75	1.10
21. $Zr_{46.75}Ti_{8.25}Cu_{7.5}Ni_{10}Be_{27.5}$	1.648	0.359	35.2	6.845	1.83	0.96
22. $Zr_{41.2}Ti_{13.8}Ni_{10}Cu_{12.5}Be_{22.5}$	1.690	0.352	34.1	6.542	1.86	0.92
23. $Cu_{57.5}Hf_{27.5}Ti_{15}$	1.555	0.356	37.3	5.428	1.94	1.01
24. $Zr_{48}Nb_8Ni_{12}Cu_{14}Be_8$	1.705	0.367	34.3	6.146	1.95	0.93
25. $Cu_{64}Zr_{36}$	1.513	0.352	34.0	5.791	2.00	0.98
26. $Zr_{55}Al_{19}Co_{19}Cu_7$	1.900	0.352	37.6	6.438	2.20	0.90
27. $Cu_{50}Hf_{43}Al_7$	1.667	0.358	42.0	5.341	2.20	1.03
28. $Ni_{45}Ti_{20}Zr_{25}Al_{10}$	1.596	0.359	40.2	6.952	2.37	1.03
29. $Ni_{40}Ti_{17}Zr_{28}Al_{10}Cu_5$	1.615	0.349	47.3	7.453	2.59	1.09
30. $Ni_{60}Nb_{27.2}Ta_{6.8}Sn_6$	1.436	0.357	59.4	7.283	3.50	1.30
31. $Ni_{60}Nb_{35}Sn_5$	1.416	0.385	66.3	8.024	3.85	1.41
32. $Fe_{53}Cr_{15}Mo_{14}Er_1C_{15}B_6$	1.292	0.320	75.0	9.742	4.20	1.47
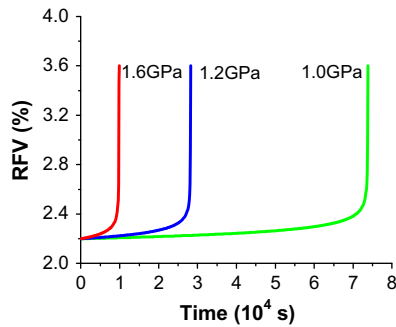
Figure 2. The evolution of x in the $Zr_{55}Ti_5Cu_{20}Ni_{10}Al_{10}$ under three different applied stresses of 1.6 GPa ($\sim\sigma_y$), 1.2 GPa ($\sim 0.8\sigma_y$), and 1.0 GPa ($\sim 0.6\sigma_y$) at room temperature.

state, and Eq. (1) is no longer valid because it fails to take into account the thermal production of the free volume or flow defect [10,19].

In the supercooled liquid state at elevated temperatures, the rate equation governing flow defect $c_f = \exp(-\frac{1}{x})$ was given by [19].

$$\dot{c}_f = -k_r c_f(c_f - c_{f,eq}) + \alpha_x \dot{\varepsilon} c_f \ln^2 c_f \qquad (3)$$

where k_r is a temperature-dependent rate constant, $c_{f,eq}$ is the equilibrium concentration of defects at a given temperature, α_x is the creation factor giving the propor-

tion between plastic strain and flow defect concentration, and

$$\dot{\varepsilon} = 2c_f f \sin h\left(\frac{\tau V}{2kT}\right) \exp\left(-\frac{\Delta G^m}{kT}\right)$$
$$= \dot{\varepsilon}_0 c_f \sinh\left(\frac{\sigma V}{2\sqrt{3}kT}\right) \qquad (4)$$

is the strain rate during homogeneous deformation with V the activation volume [10,19].

There are only limited high-temperature data, here we take $k_r = 2.3 \times 10^{10}$ s^{-1}, $\alpha_x = 0.02$, $\dot{\varepsilon}_0 = 2.8 \times 10^8$ s^{-1}, and $V = 160$ Å^3 of the $Zr_{52.5}Al_{10}Cu_{27}Ti_{2.5}Ni_8$ ($T_g \sim 663$ K) at 683 K from Ref. [20] to solve Eq. (3) numerically and the results are plotted in Figure 3. The initial value of RFV is set as 2.4%, i.e., x_C, corresponding to the elevated temperature region around glass transition temperature. At low stresses, x grows steadily at the beginning then, after a period of time, reaches a saturation value and keeps unchanged with time. The saturation value depends on the applied stress σ. A higher stress produces a larger saturation value. For the stress of 0.55 GPa, the saturation value is 4.3% and larger than that produced by the stress 0.40 GPa (3.7%). However, at a higher stress, 0.70 GPa, x grows sharply to an unreasonably large value (in excess of x_m). In this case, the MG would undergo fracture instead of homogeneous flow.
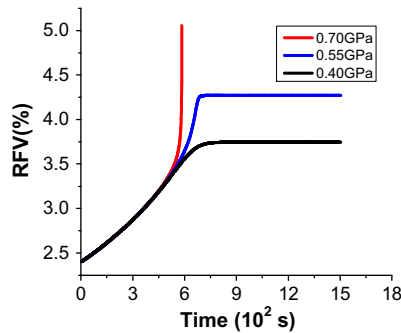
Figure 3. The evolution of RFV of $Zr_{52.5}Al_{10}Cu_{27}Ti_{2.5}Ni_8$ under three different stresses of 0.40, 0.55, and 0.70 GPa at 683 K.

When a MG sample is uniaxially compressed or stretched at room temperature and if the applied stress exceeds σ_c, x will increase to x_C at some local sites in the sample because of the statistical distribution of free volume [10]. Then, the shear flow starts at these local sites (i.e., formation of STZ), and result in the initiation and subsequent development of shear bands. The evolution of x is determined by Eq. (3) due to the temperature rise in the shear band [20,21]. A large x (thereby a large c_f) can produce a very large strain rate $\dot{\varepsilon}$ in shear band according to Eq. (4). As a result, the upper part of the sample will slide over the lower part along the shear plane. As long as there is no runaway during the sliding process, the stress would drop because the strain rate is limited by the relatively slow crosshead speed of the test machine. If the applied stress decreases below a certain value (<0.70 GPa for $Zr_{52.5}Al_{10}Cu_{27}Ti_{2.5}Ni_8$, for example) before x increases to x_m, the shear band can steadily propagate. Otherwise, the rapid increase and the ensuing concentration of free volumes will lead to the formation of nanovoids and the subsequent coalescence of these voids forms a crack [22,23]. On the other hand, if the x value of the shear front annihilates below x_C, the shear band would be arrested. Thus, if x_m of a MG is very close to x_C, the MG would exhibit a brittle fracture once it yields. As an evidence, liquid-like droplets and vein pattern often appear on the fracture surface of tough MG (e.g., Zr-MG), but they are hardly found on that of brittle MG (e.g., Mg-MG) [3]. This suggests that the Zr-MG has a smaller viscosity η in shear band than that of the Mg-MG, consistent with the fact that Zr-MG has a larger x_m as compared to that of Mg-MG according to $\eta \propto \exp(1/x)$ [10].

In summary, a critical RFV value of $x_C \sim 2.4\%$ for the onset of yielding is universally obtained in both brittle and plastic MGs, and the corresponding stress σ_c to produce such a free volume concentration is found to be less than the experimentally measured macroscopic yield stress σ_y. The deforming behavior of MGs is determined by the evolution of RFV, and specifically the relationship between the material-independent value x_C and the material-dependent value x_m at melting.

[1] J. Schroers, W.L. Johnson, Phys. Rev. Lett. 93 (2004) 255506.
[2] J. Das, M.B. Tang, K.B. Kim, R. theissmann, F. Baier, W.H. Wang, J. Eckert, Phys. Rev. Lett. 94 (2005) 205501.
[3] C.A. Schuh, T.C. Hufnagel, U. Ramamurty, Acta Mater. 55 (2007) 4067.
[4] K.W. Park, C.M. Lee, M. Wakeda, Y. Shibutani, M.L. Falk, J.C. Lee, Acta Mater. 56 (2008) 5440.
[5] G.E. Dieter, Mechanical Metallurgy, McGraw-Hill, Maidenhead, 1988.
[6] Y.H. Liu, G. Wang, R.J. Wang, D.Q. Zhao, M.X. Pan, W.H. Wang, Science 315 (2007) 1385.
[7] T. Mukai, T.G. Nieh, Y. Kawamura, A. Inoue, K. Higashi, Intermetallics 10 (2002) 1071;
H.M. Chen, S.X. Song, J.C. Huang, H.S. Chou, J.S.C. Jang, T.G. Nieh, Appl. Phys. Lett. 94 (2009) 141914;
S.X. Song, T.G. Nieh, Intermetallics 17 (2009) 762.
[8] K.W. Park, C.M. Lee, H.J. Kim, J.C. Lee, Mater. Sci. Eng. A 499 (2009) 529.
[9] B. Yang, C.T. Liu, T.G. Nieh, Appl. Phys. Lett. 88 (2006) 221911.
[10] F. Spaepen, Acta Metall. 25 (1977) 407.
[11] A.S. Argon, Acta Metall. 27 (1979) 47.
[12] W.L. Johnson, K. Samwer, Phys. Rev. Lett. 95 (2005) 195501.
[13] D. Pan, A. Inoue, T. Sakurai, M.W. Chen, Proc. Natl. Acad. Sci. USA 105 (2008) 4769.
[14] C. Nagel, K. Rätzke, E. Schmidtke, J. Wolff, U. Geyer, F. Faupel, Phys. Rev. B 57 (1998) 10224.
[15] J.F. Li, D.Q. Zhao, W.H. Wang, Appl. Phys. Lett. 93 (2008) 171907.
[16] W.H. Wang, J. Appl. Phys. 99 (2006) 093506;
W.H. Wang, J. Non-Cryst. Solids 351 (2005) 1481.
[17] S. Li, R.J. Wang, M.X. Pan, D.Q. Zhao, W.H. Wang, J. Non-Cryst. Soilds 354 (2008) 1080.
[18] Q. Luo, W.H. Wang, J. Non-Cryst. Soilds 355 (2009) 759;
Q. Luo, D.Q. Zhao, M.X. Pan, W.H. Wang, Appl. Phys. Lett. 89 (2006) 081914.
[19] P.D. Hey, J. Sietsma, A.V.D. Beukel, Acta Mater. 46 (1998) 5873.
[20] M. Bletry, P. Guyot, Y. Bréchet, J.J. Blandin, J.L. Soubeyroux, Acta Mater. 55 (2007) 6331.
[21] J.J. Lewandowski, A.L. Greer, Nat. Mater. 5 (2006) 15.
[22] B. Yang, M. Morrison, P.K. Liaw, C.T. Liu, R.A. Buchanan, T.G. Nieh, J. Mater. Res. 21 (2006) 915.
[23] W.J. Wright, T.C. Hufnagel, W.D. Nix, J. Appl. Phys. 93 (2003) 1432.